HHS Public Access

Author manuscript

Circ Heart Fail. Author manuscript; available in PMC 2020 April 01.

Published in final edited form as:

Circ Heart Fail. 2019 April ; 12(4): e005565. doi:10.1161/CIRCHEARTFAILURE.118.005565.

Sacubitril/valsartan decreases cardiac fibrosis in left ventricle pressure overload by restoring PKG signaling in cardiac fibroblasts

Ryan M. Burke, Ph.D.[1], **Janet K. Lighthouse, Ph.D.**[1], **Deanne M. Mickelsen, B.S.**[1], and **Eric M. Small, Ph.D.**[1,2,3,4,*]

[1]Aab Cardiovascular Research Institute, Department of Medicine, University of Rochester School of Medicine and Dentistry, Rochester, NY, USA.

[2]Department of Medicine, School of Medicine and Dentistry, University of Rochester, Rochester, NY 14642.

[3]Department of Pharmacology and Physiology, School of Medicine and Dentistry, University of Rochester, Rochester, NY 14642.

[4]Department of Biomedical Engineering, University of Rochester, Rochester, NY 14642.

Abstract

Background: Heart failure (HF) is invariably accompanied by development of cardiac fibrosis, a form of scarring that increases muscular tissue rigidity and decreases cardiac contractility. Cardiac fibrosis arises from a pathological attempt to repair tissue damaged during maladaptive remodeling. Treatment options to block or reverse fibrosis have proven elusive. Neprilysin is an endopeptidase that degrades vasoactive peptides, including atrial natriuretic peptide (ANF). Thus, neprilysin inhibition reduces hypertension, ultimately limiting maladaptive cardiac remodeling. LCZ696, which consists of an angiotensin receptor blocker (valsartan) and a neprilysin inhibitor (Sacubitril) was shown to be well-tolerated and significantly reduced the risk of death and hospitalization in HF patients with reduced ejection fraction. We hypothesized sacubitril / valsartan (SAC/VAL) directly inhibits fibroblast activation and development of pathological fibrosis.

Methods/Results: We utilized a mouse model of left ventricle pressure overload coupled to *in vitro* studies in primary mouse and human cardiac fibroblasts (CF) to study the impact of SAC/VAL on CF activation and cardiac fibrosis. SAC/VAL significantly ameliorated pressure overload-induced cardiac fibrosis by blocking CF activation and proliferation, leading to functional improvement. Mechanistically, the beneficial impact of SAC/VAL at least partially stemmed from restoration of protein kinase G (PKG) signaling in HF patient-derived CF, which inhibited Rho activation associated with myofibroblast transition.

Conclusions: This study reveals SAC/VAL acts directly on CF to prevent maladaptive cardiac fibrosis and dysfunction during pressure overload-induced hypertrophy, and suggests SAC/VAL

*Corresponding author, Eric M. Small, Ph.D., Aab Cardiovascular Research Institute, University of Rochester Medical Center, 601 Elmwood Avenue, Box CVRI, Rochester, NY 14642, Phone: (585) 276-7707, Fax: (585)276-9829, eric_small@urmc.rochester.edu.

should be evaluated as a direct anti-fibrotic therapeutic for conditions such as HF with preserved ejection fraction (HFpEF).

Introduction

Heart failure (HF) is the leading cause of death worldwide: the current 5-year mortality following diagnosis of HF is 50%, and the 1-year mortality for those with end-stage disease is 50%[1, 2]. In the U.S. alone, ~5.7 million people suffer from HF at a cost of $37.2 billion[2]. The progression of HF stems, in part, from the development of cardiac fibrosis[3]. Fibrosis is a form of scarring that increases the rigidity of muscular tissue, decreases cardiac contractility and can lead to lethal arrhythmias. Cardiac fibrosis arises from the aberrant, persistent stimulation of fibroblasts in a pathological attempt to repair tissue that is damaged during maladaptive remodeling[4–7]. Although current therapeutic strategies for patients in HF are primarily aimed at stimulating contractility and reducing vasoconstriction, without a complimentary approach to block or reverse the development of fibrosis, treatment options often represent a bridge to cardiac transplantation.

Angiotensin-converting enzyme (ACE) inhibitors (including enalapril) are the current standard of care for HF, demonstrating a consistent reduction in risk of death[8, 9]. Angiotensin-receptor blockers (ARBs) are used when the patient cannot tolerate ACE inhibitors, although the effect on clinical endpoints has been less consistent[10, 11]. Development of a combination therapy that increases the efficacy of ARBs would expand clinical options in the case that ACE inhibitors are contraindicated. To this end, the inhibition of vasoactive peptides has been of interest. Neprilysin is an endopeptidase that degrades various vasoactive peptides, including atrial natriuretic peptide (ANF) and brain natriuretic peptide (BNP). Thus, neprilysin inhibition in concert with an ARB reduces hypertension - ultimately limiting maladaptive cardiac remodeling. A first-in-class combination drug consisting of an ARB (valsartan) and the neprilysin inhibitor LBQ657 (Sacubitril) was recently shown to be well-tolerated, reducing blood pressure without significant angioedema in human studies[12]. Importantly, a double-blind randomized trial (PARADIGM-HF) comparing enalapril to the Novartis compound LCZ696 (or SAC/VAL) was conducted in HF patients with reduced ejection fraction, showing that LCZ696 was superior to enalapril in reducing risks of death and hospitalization[13].

While LCZ696 certainly has vasodilatory effects, it is possible there are direct and/or indirect effects of this combination therapy on the development of fibrosis. Angiotensin-II (AngII) signaling leads to the development of fibrosis indirectly via blood pressure modulation and directly via fibroblast activation[14]. Indeed, the ARB losartan causes regression of cardiac fibrosis and improved diastolic function independent of reduced blood pressure[15, 16]. Another study has also established a potentially direct antifibrotic role for BNP in the remodeling ventricle; BNP null mice displayed a significant increase in focal fibrotic lesions within the ventricle in a mouse model of pressure overload[17]. Evaluation of the effect of SAC/VAL in a rat model of myocardial infarction demonstrated reduced perivascular fibrosis and improved cardiac function[18]. This study confirmed that valsartan inhibited fibrosis *in vitro*; however, the direct effect of SAC/VAL on CF was not studied in this context.

CF express all three natriuretic peptide receptors (*Npr1*/NPRA, *Npr2*/NPRB, and *Npr3*/NPRC), and as such are expected to respond functionally to elevations in ANF by elevating cyclic guanosine monophosphate (cGMP) levels[19]. Of these receptors, NPRA binds both ANF and BNP and is the receptor most closely associated with canonical natriuretic peptide signaling via cGMP and PKG. NPRA, as well as its congeners, undergoes ligand-mediated internalization and sequestration via clathrin-mediated pathways[20]. There is complicated cross-talk between ANF, TGF-β1, AngII, and cGMP that regulates NPRA expression both at the gene and protein level as well as its guanylate cyclase activity, and these mechanisms are not fully understood in the context of disease[21–26]. It is conceivable, therefore, that SAC/VAL might exert protective effects via this ANF-NPRA-PKG signaling axis.

We conducted a preclinical trial to evaluate the role of SAC/VAL in the direct inhibition of cardiac fibrosis. We found that SAC/VAL was more effective than the molar equivalent dose of valsartan at reducing cardiac hypertrophy, diastolic dysfunction, and cardiac fibrosis in a mouse model of pressure overload-induced heart failure. We found that SAC/VAL decreased the total number of fibroblasts present in the heart and altered their genetic program in a manner consistent with a more quiescent, less activated phenotype. *In vitro* studies revealed that while valsartan acts primarily against TGF-β1/AngII-induced CF proliferation, addition of Sacubitrilat (the active metabolite of the neprilysin inhibitor in SAC/VAL) inhibited activation and myofibroblast transition. The anti-fibrotic effect of SAC/VAL is at least partially due to the inhibition of Rho signaling via stabilization of ANF-induced PKG signaling. Taken together, the results of this study shed light on potential mechanisms of SAC/VAL efficacy in heart failure with reduced ejection fraction via acting on CF.

Methods

The authors declare that all supporting data are available within the article and its online supplementary files.

Animal husbandry and transverse aortic constriction surgery

All animal studies were approved by the University of Rochester Medical Center Animal Care and Use Committee. C57Bl6/J males (Jackson Laboratories, Bar Harbor, ME) were purchased at 8 weeks of age and raised to 12 weeks of age in the vivarium facility with *ad libitum* access to standard chow and water. Mice were anesthetized with 2.0% isoflurane, placed on a heated surgical board, and given subcutaneous 2.5 mg/kg flunixin (Banamine™). After hair removal, a midline cervical incision was made to expose the trachea. A 22-gauge (PE 90) plastic intubation catheter was noninvasively inserted through the mouth and advanced into the trachea; proper placement was viewed through the cervical incision. The catheter was connected to a volume-cycled ventilator supplying supplemental oxygen with a tidal volume of 225–250 μl and a ventilation rate of 120–130 strokes/min. Surgical-plane anesthesia was subsequently maintained with 1–1.5% isoflurane. The cervical incision was closed with Vicryl 6–0 suture. A left thoracotomy was performed as follows: Skin was incised and chest cavity opened at the level of the 2nd intercostal space. A transverse section of the aorta (between the innominate and left carotid arteries) was isolated. TAC was created by placing a 6.0 silk ligature securely around the transverse aorta

and a 27-gauge needle, causing complete occlusion of the aorta. The needle was then removed, restoring a lumen with severe stenosis. Lungs were reinflated, and the chest was closed with Vicryl 6–0 suture. Muscle and skin were sutured with Vicryl 6–0 suture in a running subcuticular pattern. After returning to independent breathing, the mouse was removed from the ventilator and allowed to recover in a clean cage on a heated pad. Buprenorphine was provided every 12 hours for 72 hours post-surgery in accordance with the University Committee on Animal Research guidelines.

Drug administration

Human patients receive a target dose of 97/103 mg (Sacubitril/Valsartan) twice daily when prescribed LCZ696 (~5mg/kg/day for 80kg patient). Valsartan and sacubitril dissociate in aqueous medium and sacubtril is metabolized in vivo to the Neprilisin inhibitor LBQ657. The SAC/VAL used in our animal studies was obtained from Novartis (Basel, Switzerland) and is the identical formulation of LCZ696. However, the selection of appropriate dosing of LCZ696 in non-human species introduces several challenges due to factors such as differential intrinsic potencies of valsartan and LBQ657 for the human vs. the animal target receptor (angiotensin II type-1 (AT1)) and enzyme (NEP), differential pharmacokinetics, and differential inter-species rates/levels of hydrolysis of sacubitril prodrug to the active LBQ657. Dosing was based on Pharmacokinetics and Pharmacodynamics studies demonstrating optimal dosages required to increase ANP immunoreactivity in plasma (readout of neprilysin inhibition) and Renin concentration (AT1 receptor inhibition)[27]. Published doses of valsartan in mice are typically in the range of 10–50 mg/kg/day, which inhibit AT1 and Neprilisin. Two studies have been published to date with oral gavage dosing of LCZ696 (6 and 60 mg/kg/day, respectively) in mice[28, 29]. However it is not clear whether the impact on AT1 receptor activity and neprilysin inhibition is equivalent to that observed in humans with currently available data. For animal experiments we initially used 114 mg/kg/day LCZ696 (consisting of 52 mg/kg/day of valsartan and 62 mg/kg/day of sacubitril). Following experimental evidence regarding toxicity (likely gastritis) at 114 mg/kg/day LCZ696, and further consultation with Novartis, we reduced dosing to 57 mg/kg/day LCZ696. The comparable equimolar dose of valsartan (26 mg/kg/day, also called 1X or “low dose”) used for the remainder of the experiments matches the plasma exposure of valsartan achieved by administering 57 mg/kg/day LCZ696. 52mg/kg/day valsartan used as comparator in initial studies did not lead to toxicity and was retained as a 2X molar equivalent comparator (also called “high dose”), reflecting twice the plasma exposure of valsartan achieved with 57 mg/kg/day LCZ696. Drugs and saline controls were administered by twice daily oral gavage at 2 mL/kg/dose. Solutions were sterile filtered prior to gavage. Gavage was performed as normal the day prior to TAC surgery, skipped on the day of the surgery to allow the animals recovery time. Twice-daily gavage resumed on Day 1 post-operation and was continued throughout the remainder of the 28-day period.

Echocardiography and blood pressure analysis

Echocardiographic analysis was performed using a Vevo2100 echocardiography machine (VisualSonics, Toronto, Canada) and a linear-array 40MHz transducer (MS-550D). LV systolic and diastolic measurements were captured in M-mode from the parasternal short axis. Tissue Doppler was used to measure diastolic dysfunction in a subset of mice at Day

28. All echocardiography was performed in a blinded fashion. Systolic/diastolic blood pressure and resting heart rate were evaluated by a non-invasive tail cuff plethysmograph, on which mice were trained prior to measurements (Visitech Systems, Apex, NC).

RNA isolation from whole hearts

Mouse ventricular fibroblasts were isolated by Langendorff perfusion. Briefly, the heart was removed from the animal and the aorta cannulated and secured on a blunted 21G needle and the heart digested with 1 mg/mL collagenase II (305U/μg, Worthington Biochemicals, Lakewood, NJ) as described previously[30]. The ventricular tissue was then removed from the cannula, shredded using forceps, and passed through a 100μm filter to obtain a single cell suspension. The cardiomyocytes were separated by gravity sedimentation for 12 minutes at 37°C and then the remaining supernatant was centrifuged at 1000rpm for 5 minutes at 4°C to pellet the non-myocyte population. Cardiac fibroblasts were isolated by plating the resuspended pellet for 2 hours at 37°C and washing the attached cells (fibroblasts) three times with phosphate-buffered saline before RNA isolation. RNA isolation was performed on CM and CF fractions using Trizol/chloroform extraction as previously described[30, 31].

qPCR and analysis

Genomic DNA was removed by treating isolated RNA samples with Turbo DNAse (Ambion/Thermo Fisher, Waltham, MA). cDNA was generated using 500–1000ng RNA for all subsequent experiments using iScript Reverse Transcriptase kit (Bio-Rad, Hercules, CA) per manufacturer's instructions. Gene expression was examined by qPCR using iQ SYBR Green Supermix (Bio-Rad, Hercules, CA) and the CFX Connect Real-Time PCR Detection System (Bio-Rad). Relative mRNA levels were normalized to ribosomal *18s* and calculated using the $2^{-(\Delta\Delta Ct)}$ method.

Histology and analysis

When fully unconscious, the mouse chest cavity was opened and the heart tissue was perfused with calcium-and magnesium-free phosphate-buffered saline (PBS), followed by fixation with 10% neutral buffered formalin solution overnight and subsequent histologic processing, paraffin embedding, and sectioning.

Fibrosis: 5 μM sections were generated at ten equally spaced levels from each heart, mounted on slides and stained with PicroSirius Red according to manufacturer instructions (Abcam, Cambridge, MA). Images were captured at 10x on a BX51 epifluorescence microscope (Olympus, Shinjuku, Japan) using circularly polarized light to generate a birefringent (red/thick, green/thin) signal from collagen fibers. To evaluate fibrosis, areas of interest (epicardial, perivascular, and interstitial) were defined in ImageJ (NIH). The extent of epicardial fibrosis was determined by the number of positive pixels in the green and red channels in an area defined by a freehand line along the epicardium extended in 100 pixels from the epicardial surface, divided by the arc length of the epicardial freehand line. The extent of perivascular fibrosis was determined by calculating the ratio of the area of the positive pixels surrounding the vessel to the total vessel area. The extent of interstitial fibrosis was determined by calculating the number of positive pixels in the non-epicardial,

non-perisvascular area of the section and dividing by the total non-epicardial, non-perivascular area.

Cardiomyocyte hypertrophy: To evaluate the extent of cardiomyocyte hypertrophy, sections were stained with DAPI (to visualize nuclei, 350/50ex-460/50em) and wheat germ agglutinin (to visualize cell borders, 620/60ex-700/75em) scanned at 20x on a BX70 confocal microscope (Olympus, Shinjuku, Japan). No less than 250 transverse myocytes per animal were evaluated for cross-sectional area.

Assessment of non-myocyte population: Sections were stained with DAPI (to visualize nuclei), Alexa 488-conjugated isolectin-B4 (Sigma-Aldrich, St. Louis, MO), and rabbit-anti-vimentin (Abcam, Cambridge, MA) followed by a donkey-anti-rabbit secondary antibody conjugated to Alexa 594 (Invitrogen, Carlsbad, CA)[30, 31]. $DAPI^{+}/IB4^{-}/vimentin^{+}$ cells were counted in 3 sections per animal. To confirm resident CF populations, PDGFRα staining was also included[32, 33]. Dilutions in Supplementary Table 1.

Primary cell isolation – mouse

Neonatal mouse CF were isolated as previously described[30]. Briefly, Primary CFs were isolated from neonatal mouse hearts by differential plating. Hearts were removed from neonatal mice on the day of birth. Ventricles were isolated and transferred to a solution of 0.8 mg/mL collagenase type II (Worthington Labs) and finely minced. Hearts were then agitated in 10 mL of collagenase solution in four cycles of 10 min each, collecting cells at each step by centrifugation. Cells were strained through a 70-μm filter and plated on a 10-cm dish for 1 h to enrich adherent cells (nonmyocyte fraction).

Primary cell isolation – human heart failure

CF were isolated from patient-derived tissue as previously published[30], following written informed consent under the auspices of an approved University of Rochester IRB protocol (#52958). Briefly, left ventricle tissue that would normally be discarded during ventricular assist device (VAD) implantation was freshly obtained and dissociated using a heated (37 °C) gentle-MACS Octo dissociator (Miltenyi Biotec) with an enzymatic dissociation system (Neonatal Heart Dissociation Kit; Miltenyi Biotec). The resulting cells were sedimented as described in the neonatal isolation and expanded for two passages before freezing. CFs were maintained in high-glucose DMEM supplemented with 1% penicillin–streptomycin and 10% FBS. CFs were used between passages 3 and 7 for experiments, with days to passage and passage number recorded.

Western blotting/immunoprecipitation and analysis

Western blotting was performed as previously described[30, 34]. A list of primary and secondary antibodies, including manufacturer number and working concentration, may be found in Supplementary Table 1. Immunoprecipitation to detect activated RhoA was performed using a pulldown assay kit (Cytoskeleton, Inc.) according to manufacturer instructions.

Statistical analysis

Statistics were performed with Prism 7 (GraphPad). Statistical analyses and experimental replicates are listed individually in the figure legends. Replicates in this study are biological (not technical) unless specifically noted otherwise.

Results

SAC/VAL is more effective than molar equivalent valsartan at preserving cardiac function in a mouse model of pressure overload-induced heart failure

To gauge the efficacy of SAC/VAL at preserving systolic cardiac function in the context of direct comparison to valsartan therapy alone, we used the transverse aortic constriction (TAC) model of pressure overload-induced heart failure in adult male C57Bl6/J animals (experimental timeline in Supplementary Figure 1A). TAC surgery results in a reproducible increase in aortic flow velocity (Supplementary Figure 1B) and in pressure gradient between the aorta and heart (Supplementary Figure 1C) due to the establishment of aortic stenosis. Four treatment regimens were compared: saline, 57 mg/kg SAC/VAL, 26 mg/kg valsartan (equimolar, or “low dose”), 52 mg/kg valsartan (2x molar equivalents, or “high dose”). 26 mg/kg valsartan and 57 mg/kg SAC/VAL represent molar equivalents of valsartan (the only difference between these regimens is the presence of Sacubitril). Animal survival was not significantly different amongst treatment groups with the exception of 52 mg/kg valsartan (Supplementary Figure 1D), and body weight was not significantly altered by treatment regimen (Supplementary Figure 1E). Both high dose valsartan (at 15 and 28 days) and the SAC/VAL (at 28 days) regimens resulted in a significant decrease in systolic blood pressure (Supplementary Figure 1F), but no significant alterations to resting heart rate (Supplementary Figure 1G).

SAC/VAL resulted in a significant decrease in cardiac hypertrophy at 28 days post-TAC relative to both saline and the molar equivalent of valsartan (26 mg/kg), as determined by heart weight to tibia length ratio. Both SAC/VAL and 52 mg/kg (2x molar equivalents) valsartan conferred significant protection from hypertrophy (Figure 1A). This was confirmed by echocardiographic measurement of the left ventricular (LV) mass, where the SAC/VAL regimen was associated with a significantly lower LV mass than equimolar valsartan – which itself provided no significant anti-hypertrophic protection relative to the saline control (Figures 1B and 1C). None of the regimens significantly affected kidney weight to tibia length ratio (Supplementary Figure 1H), suggesting alterations to the blood pressure were not due to major changes in renal function. SAC/VAL is associated with significant decreases in systolic and diastolic internal dimension relative to the molar equivalent of valsartan (Figures 1D–E) beginning at 14 days and persisting throughout the experiment. SAC/VAL is also associated with significant decreases in systolic and diastolic volume relative to the molar equivalent of valsartan (Figures 1F–G) beginning at 21 days. Consequently, SAC/VAL is also associated with significant improvements relative to equimolar valsartan in the systolic functional parameters fractional shortening (Figure 1H) and ejection fraction (Figure 1I) at the 28-day time point. SAC/VAL and 52 mg/kg valsartan regimen (2x molar equivalent) both provide significant functional improvement beginning at 14 days. Furthermore, SAC/VAL is associated with significant decrease in cardiomyocyte

(CM) cross-sectional area, as is the 2x valsartan regimen (Figures 1J–K). CM isolated by Langendorff perfusion reveal that SAC/VAL treatment is associated with significant suppression of fetal gene re-expression (*Acta1*, *Myh7*), retention of *Myh6* expression, and reduced expression of natriuretic peptides ANF and BNP (*Nppa*, *Nppb*) relative to the molar equivalent of valsartan (Supplementary Figure 2).

SAC/VAL is more effective than valsartan at ameliorating cardiac fibrosis, with distinct effects on cardiac fibroblast gene expression

The effect of SAC/VAL on diastolic function was measured by E/A ratio and E/E' ratio, which represent distinct indices of diastolic dysfunction (E/A in early dysfunction, E/E' in more established disease). E/A was not statistically significantly changed by SAC/VAL relative to the molar equivalent of valsartan at the terminal time point (Figure 2A), while E/E' values from both the intraventricular septum and the mitral valve revealed a trend ($p = 0.11$ and 0.06 respectively) toward SAC/VAL-conferred protection from diastolic dysfunction relative to equimolar valsartan alone (Figure 2B). Diastolic dysfunction is associated with increasing stiffness and fibrotic deposition, suggesting that SAC/VAL may modulate cardiac fibrosis more efficiently than the molar equivalent of valsartan. In keeping with the E/E' ratio, we found that hearts from mice treated with the SAC/VAL regimen were significantly less fibrotic than were those treated with the molar equivalent of valsartan (Figure 2C). Polarized light imaging of PicroSirius Red-stained sections revealed significant decreases in epicardial and interstitial fibrosis (Figures 2D–F). Both thin (green) and thick (red) fibers were affected, with no observable shift from thick to thin or vice versa. In contrast, there appeared to be no significant effect of SAC/VAL relative to the valsartan equivalent in perivascular fibrosis. Interestingly, 52 mg/kg valsartan (2x molar equivalent) was associated with significant protection from fibrosis (thin and thick fibers) in all three areas of interest. We hypothesized that the extent of fibrosis might best correlate with the number of fibroblasts in the heart (extent of fibroblast population expansion). Therefore, we stained for PDGFRα and vimentin, two markers of resident mesenchymal cells/cardiac fibroblasts (Figure 3A, B). We found that while low dose valsartan led to a minor reduction in PDGFRα and vimentin^{+} fibroblasts found in the heart post-TAC relative to saline, SAC/VAL was associated with a significant decrease in fibroblast population, displaying significantly less PDGFRα positivity than the molar equivalent of valsartan (Figures 3C, D). Endothelial cells, which can also express vimentin, did not appear to be affected by drug regimens in terms of total capillary area (Supplementary Figures 3A–B), but average intercapillary distance within the transverse myocardium reflected the modulation in CM size shown in Figures 1J–K (Supplementary Figure 3C). CF isolated from the hearts via Langendorff perfusion reveal that SAC/VAL treatment is associated with gene expression profiles consistent with decreased myofibroblast transition/activation (low *Acta2* and *Postn*), lower proliferation (low *Ccna2*, *Ccne1*, *Sprr2b*; high *Cdkn1a*), improved protection from oxidative damage (high *Mt1*), and decreased production of ECM molecules (low *Col1a1*, *Col3a1*, *Fn*) compared to saline treated controls (Figure 3E). High dose valsartan was also associated with these significant alterations in gene expression (and the addition of a significant increase in *Tcf21*, a potential marker of quiescent fibroblasts)[35]. However, the molar equivalent valsartan regimen failed to confer any statistically significant changes in gene expression in CF relative to saline controls – again indicating that SAC/VAL

measurably improves upon equimolar valsartan as a cardiac therapeutic in the pressure overload model, with specific anti-fibrotic effects that are not solely attributable to the valsartan portion of the molecule.

The neprilysin inhibitor Sacubitrilat targets myofibroblast activation in vitro

To further investigate the effects of SAC/VAL on CF as compared to valsartan, we undertook studies in neonatal mouse CF (nCF) cultures. We found that pre-treatment of nCF with increasing concentrations of ANF conferred a dose-dependent inhibition of *Acta2* gene expression induced by 10 ng/mL TGF-β1 (Figure 4A). We confirmed this by recreating the experiment (this time including an unstimulated negative control) and assaying for the *Postn* and *Tcf21* expression (Figures 4B–C). In each case, increasing doses of ANF pretreatment inhibited *Postn* and partially restored *Tcf21* expression. A third iteration of this experiment revealed that the effect of ANF on activation/quiescence genes do not extend to cell cycle/proliferation-associated genes, which are unresponsive to ANF in these experiments (Figure 4D). This was confirmed by adding AngII to the stress stimulus (10 ng/mL TGF-β1 / 1 μM AngII), which resulted in significantly increased expression of the mitosis-associated genes *Ccna2* and *Cdk1*, and significantly lower expression of the cell cycle inhibitor *Cdkn1a* – consistent with the ability of AngII to stimulate CF proliferation (Figure 4E)[30]. Again, addition of ANF did not significantly alter cell cycle/proliferation gene expression, but did significantly impair gene expression associated with myofibroblast transition and activation (*Acta2, Col1a1, Postn*). Taken together, this set of experiments suggests that ANF signaling predominantly inhibits the gene program that signifies myofibroblast transition, while angiotensin signaling predominantly induces the gene program that signifies fibroblast proliferation. This is consistent with the dual function of SAC/VAL as a neprilysin inhibitor (inhibition of ANF degradation, potentiation of ANF signaling) and as an angiotensin receptor blocker (inhibition of AngII signaling).

To directly evaluate the effects of Sacubitril versus valsartan, we made use of the activated form of Sacubitril (Sacubitrilat). Sacubitril has been shown to be converted to Sacubitrilat by the liver in a CES1-dependent manner[36]. Interestingly, nCF express *Ces1*, and this expression is insensitive to stress stimuli – suggesting the possibility of direct conversion of Sacubitril to Sacubitrilat in CF (Supplementary Figure 4). To assess the effects of Sacubitrilat on nCF exposed to stress stimuli, we repeated the experiment shown in Figure 4E, adding a condition in which 200 μM Sacubitrilat was added to the ANF pre-treatment (Figure 5A). Sacubitrilat was associated with significant decreases in *Col1a1* and *Postn* relative to ANF pre-treatment alone, as was expected. Unexpectedly, pre-treatment with Sacubitrilat was also associated with significant inhibition of cell cycle/proliferation-associated gene expression. To determine whether these effects were specific to Sacubitrilat, we repeated the experiment, comparing how addition of valsartan (200 μM) and valsartan/Sacubitrilat (200 μM each, SAC/VAL mimic) to the pre-treatment regimen compared to pre-treatment with ANF alone. Figure 5B shows that while valsartan pre-treatment generally had few effects on nCF gene expression relative to ANF pre-treatment alone (the exception was a significant decrease in *Ccna2* expression), combining valsartan and Sacubitrilat in pre-treatment resulted in significant decreases in *Acta2, Col1a1*, and *Postn* (myofibroblast transition/activation genes) coupled to inhibition of cell cycle genes (significantly lower

Ccna2 and *Cdk1*, significantly higher *Cdkn1a*). To confirm that the significant changes in gene expression were mirrored at the protein level, we repeated the experiment and performed a Western blot for ACTA2, which was significantly decreased by the combination of Sacubitrilat and valsartan at 24 hours (Figure 5C).

Sacubitrilat-mediated protection from myofibroblast transition is mediated by PKG-dependent inhibition of RhoA activation

We next asked whether sacubitrilat activity in nCF is via stabilizing ANF-natriuretic peptide receptor (NPR)-cGMP-PKG signaling. To do this, we made use of the vasodilator-stimulated phosphoprotein (VASP), which is phosphorylated at S239 with greater affinity by PKG than PKA, which preferentially phosphorylates S157[37]. Again, cells were pretreated with ANF, in the presence or absence of valsartan or Sacubitrilat, then stimulated with TGF-β1/AngII to simulate stress. We found that Sacubitrilat or the combination of valsartan and Sacubitrilat potentiates VASP-pS239, while valsartan alone does not (Figures 6A–B). To confirm that Sacubitrilat activity is predominantly transduced through cGMP/PKG, we made use of the indolocarbazole PKG inhibitor KT5822 (20 nM)[38]. In the absence of KT5822, we confirmed again that ANF-induced, PKG-dependent induction of VASP-pS239 was potentiated by Sacubitrilat and not valsartan (Figures 6C–D). In the presence of KT5822, VASP-pS239 was completely lost in all conditions but the Sacubitrilat treatment, which is itself significantly decreased from the degree of VASP-pS239 present in the Sacubitrilat-treated nCF without KT5822 (see Discussion). This result confirms that PKG is required for Sacubitrilat-induced signaling in nCF, which implies that ANF and the natriuretic peptide receptor pathway are indeed the operative signaling pathway that confers protection from myofibroblast transition.

To more closely explore the relationship between the potentiation of PKG signaling by Sacubitrilat and its observed effects on inhibition of the signals that lead to myofibroblast transition, we focused on a protein called Ras homolog gene family member A (RhoA). RhoA is activated by TGF-β1, and initiates signaling pathways that induce stress fiber formation and the acquisition of mesenchymal properties[39]. Furthermore, inhibitors of RhoA effector molecules such as ROCKs have been evaluated in clinical trials targeting pulmonary arterial hypertension – also a disease involving significant organ remodeling[40]. RhoA is known to be phosphorylated by PKG at S188, which inhibits RhoA cytoskeletal reorganization functions while simultaneously protecting it from ubiquitination and subsequent proteasomal degradation[41]. We confirmed that Sacubitrilat treatment potentiates RhoA-pS188 in nCF under the same conditions evaluated for VASP-pS239 (Figures 6E–F).

To determine the degree of RhoA functional inhibition in a clinically relevant manner, we evaluated CF isolated from five heart failure (HF) patients that had undergone left ventricular assist device (LVAD) implantation (termed HFCF). We characterized mRNA and protein from these HFCF (unstimulated or stimulated with TGF-β1/AngII), finding that myofibroblast markers were induced by TGF-β1/AngII in four of the five patient-derived lines (Supplementary Figures 5–6). HFCF were subjected to pre-treatment with vehicle, TGF-β1/AngII/ANF (T/A/A, positive control for stress), T/A/A/Y-27632 (ROCK inhibitor, downstream of Rho), T/A/A/Sacubitrilat, T/A/A/valsartan, and T/A/A/valsartan/Sacubitrilat. We assayed for protein levels of NPRA (the primary receptor for ANF), PKG1A (the

catalytic subunit of PKG), and ACTA2 (measure of myofibroblast transition). We found that for all non-vehicle conditions, NPRA expression was repressed relative to vehicle – consistent with literature and ruling out possible effects on NPRA recycling and stability (Supplementary Figure 6)[20, 25]. Notably, NPRA protein expression was recovered in any patient-derived line save VAD2, which was a notable outlier in all other measures as well. We also found that PKG1A protein levels are insensitive to these experimental manipulations in all patient-derived lines, which when combined with the evidence from the PKG inhibition experiments points to PKG activity, not expression level, as the target of SAC/VAL. We performed a co-immunoprecipitation using beads conjugated to the Rho-binding domain of rhotekin, an effector of Rho signaling. Rhotekin only binds activated (GTP-bound) Rho, which allows for the direct comparison of total Rho to activated Rho. As expected, Rho activation was not inhibited by Y-27632, which inhibits a distinct downstream effector, p160/ROCK, although all HFCF showed measurable levels of total Rho protein in response to TGF-β1/AngII/ANF (Figure 7A). However, we found that the combination of Sacubitrilat and valsartan significantly reduced Rho activation for all HFCF (Figure 7A). Interestingly, while the combination of the two component drugs of SAC/VAL always successfully decreased Rho activation, there was variability as to which component was more effective in doing so alone; VADs 1, 3, and 4 were most responsive to Sacubitrilat, and VAD2 was responsive only to valsartan (Figures 7B–E). Interestingly, there was also variability in induction of ACTA2 protein expression, as well as its inhibition by both Y-27632 and the Sacubitrilat/valsartan combination – variability that was also hinted at by the gene expression results (Supplementary Figure 5). We concluded from this set of experiments that in HFCF, the combination of Sacubitrilat and valsartan does indeed act to potentiate PKG-dependent inhibition of RhoA, a major effector of myofibroblast transition and activation. This was confirmed by the consistent decrease in ACTA2 expression in response to the combination of the two component drugs.

Discussion

LCZ696 was identified as a significant improvement over standard of care (the ACE inhibitor enalapril) in patients with class II, III, or IV heart failure and reduced ejection fraction in the PARADIGM-HF trial[42]. In the ensuing years, a healthy discussion has arisen regarding the results and design of this trial - particularly the potential for understatement of adverse event rate due to both the entry criteria for the study and the run-in period design[43]. The wealth of clinical literature regarding LCZ696 has far outpaced the knowledge of how it mechanistically operates on the cellular level particularly in CF – while valsartan's role as an AT_1R blocker is well-characterized in CF, what effects neprilysin inhibition has on CF (particularly in the context of pathological signaling) are effectively unknown.

This study was intended to dissect the role of SAC/VAL in the setting of cardiac fibrosis. We found that SAC/VAL, as expected, represented a significant advancement over equimolar "low dose" valsartan alone in protection from cardiac functional decline in a mouse model of pressure overload-induced heart failure. SAC/VAL altered the pathological state of CF, yielding a gene expression program that was more reflective of quiescence than myofibroblast activation – which valsartan at an equivalent concentration was incapable of doing. We found that while valsartan-treated animals had significantly fewer CF in the heart

at the terminal time point than did control animals, SAC/VAL-treated animals had significantly fewer CF than “low dose” valsartan-treated. *In vitro*, we were able to ascertain that both Sacubitrilat and valsartan ameliorated human patient-derived hfCF activation – and in neonatal mouse CF, Sacubitrilat predominantly modulated activation gene expression while valsartan predominantly modulated proliferation gene expression.

Interestingly, in a recent study using a rat model of myocardial infarction (MI), valsartan, not Sacubitrilat, was primarily responsible for the anti-fibrotic effects in cardiac fibroblasts[44]. There is at first an apparent disconnect between this study and ours – as we found that valsartan primarily altered proliferative capacity in the mouse CF while sacubtrilat affected myofibroblast transition and activation genes. This distinction was less clear in HFCF, where certain patient-derived lines responded better to Sacubitrilat and others to valsartan – with all lines being maximally responsive to the combination of the two. This previous study differs from ours in three important ways.

While our study made use of neonatal mouse CF, adult mouse pathological CF, and human hfCF, the other study used adult rat CF – potentially explaining some of the difference in results. Their study was also performed in MI, while ours was performed in pressure overload – and we have shown that fibroblast transcriptional responses to these disease models are distinct[30]. Their study made use of radiolabeled proline uptake to determine fibrotic synthesis, as opposed to our study which focused mainly on transcription profiles in CF. The extent of temporal overlap between the development of a gene program that induces the myofibroblast transition and the development of an activated, ECM-secreting myofibroblast is still unresolved, and the results from these two studies suggest that this might be an excellent avenue for further investigation of the fibrotic response during pressure overload.

Interestingly, both of these studies reveal direct anti-fibrotic effects of natriuretic peptide-induced signaling on cardiac fibroblasts – with their study focusing on BNP and ours on ANF. Perhaps most interesting of the results from our study was the set of findings detailing how ANF works directly on CF to promote a less activated gene expression profile. We consistently found that NPRA protein expression level was decreased in response to TGF-β1/AngII stimulus in hfCF, consistent with literature and pointing to extended ligand lifetime as opposed to stabilization of receptor protein expression as the mechanism by which Sacubitrilat promotes PKG signaling in fibroblasts. The dynamics of NPRA inactivation and downregulation are certainly an important subject for further study – not only in CF, but in all pathology-relevant cell types expressing NPRA. Simultaneously, we found that Sacubitrilat/valsartan consistently rescued heart failure patient-derived CF from pathologic levels of Rho activation, while valsartan alone had a less consistent effect. As RhoA can be inactivated by PKG-dependent phosphorylation at S188, and the increased ligand lifetime of ANF in the presence of Sacubitrilat correlated with decreased Rho activation and ACTA2 expression, our data in these patient-derived cells suggest strongly that rescue of PKG signaling by Sacubitrilat was the driving mechanism behind the decreased myofibroblast activation.

To this end, we indeed found PKG to be essential for Sacubitrilat-mediated inhibition of myofibroblast transition, confirming the requirement for NPRA guanylate cyclase activity in maintaining a non-pathologic state in CF. We observed that PKG1A (catalytic subunit) total protein levels were insensitive to stimulation with TGF-β1/AngII, suggesting that defects in NPRA/cGMP signaling in pathologic CF do indeed stem from PKG1A activity and not PKG1A protein level. However, we also found that treating CF with Sacubitrilat in the presence of the PKG inhibitor KT5822 did not fully ablate the PKG-dependent phosphorylation of VASP at S239. The incomplete inhibition of VASP-pS239 in KT5822^{+}/Sacubitrilat cells likely has two root causes. While highly specific for PKG (IC_{50} 2 nM for PKG versus 37 nM for PKA)[45], literature suggests that use of KT5822 might potentiate PKA signaling and cross-phosphorylation of PKG targets[38]. Furthermore, 20 nM KT5822 pre-treatment was chosen to inhibit PKG (2 nM IC_{50}) as much as possible, without strongly inhibiting PKA (37 nM IC_{50}) – but this dose was unlikely to fully inhibit PKG. It is possible that the addition of Sacubitrilat potentiates PKG via ANF-NPRA-cGMP strongly enough that we were able to still see VASP-pS239 even in the presence of this dose of KT5822. Regardless, potential redundancy in PKG/PKA signaling is likely to be an important clinical consideration for the use of neprilysin inhibitors in the context of heart failure.

The data from this pre-clinical trial suggest that in addition to the known positive systemic effects of promoting PKG signaling (vasorelaxation, lowered blood pressure), less obvious direct effects on cells other than smooth or cardiac muscle exist as well. In this case, we have shown that the Sacubitrilat component of SAC/VAL is capable of directly modulating PKG signaling in cardiac fibroblasts, which inhibits the expression of the myofibroblast transition-related gene program via promoting PKG-dependent inhibition of Rho-mediated signaling.

Supplementary Material

Refer to Web version on PubMed Central for supplementary material.

Sources of Funding

This study was partially funded by Investigator-Initiated Research Project grant LCZ696BUSNC04T from Novartis Pharmaceuticals (to E.M.S.). The authors were also supported by NIH/National Heart, Lung, and Blood Institute Grants R01HL133761, R01HL136179, and R01HL120919 (to E.M.S.), T32HL007937 and F32HL136066 (to R.M.B.), T32HL066988 (to J.K.L.); an American Heart Association Grant 15POST25550114 (to J.K.L.); and a Pilot Study Grant from the Aab Cardiovascular Research Institute at the University of Rochester School of Medicine and Dentistry.

Disclosures

EMS was partially supported by a grant from Novartis Pharmaceuticals.

References

1. Hunt SA, Abraham WT, Chin MH, Feldman AM, Francis GS, Ganiats TG, Jessup M, Konstam MA, Mancini DM, Michl K, Oates JA, Rahko PS, Silver MA, Stevenson LW, Yancy CW, Antman EM, Smith SC Jr., Adams CD, Anderson JL, Faxon DP, Fuster V, Halperin JL, Hiratzka LF, Jacobs AK, Nishimura R, Ornato JP, Page RL, Riegel B, American College of C, American Heart Association Task Force on Practice G, American College of Chest P, International Society for H, Lung T, Heart Rhythm S. Acc/aha 2005 guideline update for the diagnosis and management of chronic heart

failure in the adult: A report of the american college of cardiology/american heart association task force on practice guidelines (writing committee to update the 2001 guidelines for the evaluation and management of heart failure): Developed in collaboration with the american college of chest physicians and the international society for heart and lung transplantation: Endorsed by the heart rhythm society. Circulation. 2005;112:e154–235 [PubMed: 16160202]

2. Lloyd-Jones D, Adams R, Carnethon M, De Simone G, Ferguson TB, Flegal K, Ford E, Furie K, Go A, Greenlund K, Haase N, Hailpern S, Ho M, Howard V, Kissela B, Kittner S, Lackland D, Lisabeth L, Marelli A, McDermott M, Meigs J, Mozaffarian D, Nichol G, O'Donnell C, Roger V, Rosamond W, Sacco R, Sorlie P, Stafford R, Steinberger J, Thom T, Wasserthiel-Smoller S, Wong N, Wylie-Rosett J, Hong Y, American Heart Association Statistics C, Stroke Statistics S. Heart disease and stroke statistics−−2009 update: A report from the american heart association statistics committee and stroke statistics subcommittee. Circulation. 2009;119:480–486 [PubMed: 19171871]
3. Hill JA, Olson EN. Cardiac plasticity. N Engl J Med. 2008;358:1370–1380 [PubMed: 18367740]
4. Small EM. The actin-mrtf-srf gene regulatory axis and myofibroblast differentiation. J Cardiovasc Transl Res. 2012;5:794–804 [PubMed: 22898751]
5. Formation Hinz B. and function of the myofibroblast during tissue repair. J Invest Dermatol. 2007;127:526–537 [PubMed: 17299435]
6. Tomasek JJ, Gabbiani G, Hinz B, Chaponnier C, Brown RA. Myofibroblasts and mechano-regulation of connective tissue remodelling. Nat Rev Mol Cell Biol. 2002;3:349–363 [PubMed: 11988769]
7. Hinz B, Celetta G, Tomasek JJ, Gabbiani G, Chaponnier C. Alpha-smooth muscle actin expression upregulates fibroblast contractile activity. Mol Biol Cell. 2001;12:2730–2741 [PubMed: 11553712]
8. Effects of enalapril on mortality in severe congestive heart failure. Results of the cooperative north scandinavian enalapril survival study (consensus). The consensus trial study group. N Engl J Med. 1987;316:1429–1435 [PubMed: 2883575]
9. Effect of enalapril on survival in patients with reduced left ventricular ejection fractions and congestive heart failure. The solvd investigators. N Engl J Med. 1991;325:293–302 [PubMed: 2057034]
10. Cohn JN, Tognoni G, Valsartan Heart Failure Trial I. A randomized trial of the angiotensin-receptor blocker valsartan in chronic heart failure. N Engl J Med. 2001;345:1667–1675 [PubMed: 11759645]
11. Young JB, Dunlap ME, Pfeffer MA, Probstfield JL, Cohen-Solal A, Dietz R, Granger CB, Hradec J, Kuch J, McKelvie RS, McMurray JJ, Michelson EL, Olofsson B, Ostergren J, Held P, Solomon SD, Yusuf S, Swedberg K, Candesartan in Heart failure Assessment of Reduction in M, morbidity I, Committees. Mortality and morbidity reduction with candesartan in patients with chronic heart failure and left ventricular systolic dysfunction: Results of the charm low-left ventricular ejection fraction trials. Circulation. 2004;110:2618–2626 [PubMed: 15492298]
12. Kario K, Sun N, Chiang FT, Supasyndh O, Baek SH, Inubushi-Molessa A, Zhang Y, Gotou H, Lefkowitz M, Zhang J. Efficacy and safety of lcz696, a first-in-class angiotensin receptor neprilysin inhibitor, in asian patients with hypertension: A randomized, double-blind, placebo-controlled study. Hypertension. 2014;63:698–705 [PubMed: 24446062]
13. McMurray JJ, Packer M, Desai AS, Gong J, Lefkowitz MP, Rizkala AR, Rouleau JL, Shi VC, Solomon SD, Swedberg K, Zile MR, Investigators P-H, Committees. Angiotensin-neprilysin inhibition versus enalapril in heart failure. N Engl J Med. 2014;371:993–1004 [PubMed: 25176015]
14. Wynn TA, Ramalingam TR. Mechanisms of fibrosis: Therapeutic translation for fibrotic disease. Nat Med. 2012;18:1028–1040 [PubMed: 22772564]
15. Ciulla MM, Paliotti R, Esposito A, Diez J, Lopez B, Dahlof B, Nicholls MG, Smith RD, Gilles L, Magrini F, Zanchetti A. Different effects of antihypertensive therapies based on losartan or atenolol on ultrasound and biochemical markers of myocardial fibrosis: Results of a randomized trial. Circulation. 2004;110:552–557 [PubMed: 15277331]
16. Diez J, Querejeta R, Lopez B, Gonzalez A, Larman M, Martinez Ubago JL. Losartan-dependent regression of myocardial fibrosis is associated with reduction of left ventricular chamber stiffness in hypertensive patients. Circulation. 2002;105:2512–2517 [PubMed: 12034658]

17. Tamura N, Ogawa Y, Chusho H, Nakamura K, Nakao K, Suda M, Kasahara M, Hashimoto R, Katsuura G, Mukoyama M, Itoh H, Saito Y, Tanaka I, Otani H, Katsuki M. Cardiac fibrosis in mice lacking brain natriuretic peptide. Proc Natl Acad Sci U S A. 2000;97:4239–4244 [PubMed: 10737768]

18. von Lueder TG, Wang BH, Kompa AR, Huang L, Webb R, Jordaan P, Atar D, Krum H. The angiotensin-receptor neprilysin inhibitor lcz696 attenuates cardiac remodeling and dysfunction after myocardial infarction by reducing cardiac fibrosis and hypertrophy. Circulation. Heart failure. Circ Heart Fail. 2015 1;8(1):71–8. [PubMed: 25362207]

19. Pandey KN. Guanylyl cyclase/natriuretic peptide receptor-a signaling antagonizes phosphoinositide hydrolysis, ca(2+) release, and activation of protein kinase c. Front Mol Neurosci. 2014;7:75 [PubMed: 25202235]

20. Somanna NK, Pandey AC, Arise KK, Nguyen V, Pandey KN. Functional silencing of guanylyl cyclase/natriuretic peptide receptor-a by microrna interference: Analysis of receptor endocytosis. Int J Biochem Mol Biol. 2013;4:41–53 [PubMed: 23638320]

21. Fujio N, Gossard F, Bayard F, Tremblay J. Regulation of natriuretic peptide receptor a and b expression by transforming growth factor-beta 1 in cultured aortic smooth muscle cells. Hypertension. 1994;23:908–913 [PubMed: 7911451]

22. Arise KK, Pandey KN. Inhibition and down-regulation of gene transcription and guanylyl cyclase activity of npra by angiotensin ii involving protein kinase c. Biochem Biophys Res Commun. 2006;349:131–135 [PubMed: 16930545]

23. Kumar P, Arise KK, Pandey KN. Transcriptional regulation of guanylyl cyclase/natriuretic peptide receptor-a gene. Peptides. 2006;27:1762–1769 [PubMed: 16517010]

24. Kumar P, Bolden G, Arise KK, Krazit ST, Pandey KN. Regulation of natriuretic peptide receptor-a gene expression and stimulation of its guanylate cyclase activity by transcription factor ets-1. Biosci Rep. 2009;29:57–70 [PubMed: 18651838]

25. Pandey KN, Nguyen HT, Garg R, Khurana ML, Fink J. Internalization and trafficking of guanylyl (guanylate) cyclase/natriuretic peptide receptor a is regulated by an acidic tyrosine-based cytoplasmic motif gday. Biochem J. 2005;388:103–113 [PubMed: 15574117]

26. Pandey KN. Guanylyl cyclase / atrial natriuretic peptide receptor-a: Role in the pathophysiology of cardiovascular regulation. Can J Physiol Pharmacol. 2011;89:557–573 [PubMed: 21815745]

27. Gu J, Noe A, Chandra P, Al-Fayoumi S, Ligueros-Saylan M, Sarangapani R, Maahs S, Ksander G, Rigel DF, Jeng AY, Lin TH, Zheng W, Dole WP. Pharmacokinetics and pharmacodynamics of lcz696, a novel dual-acting angiotensin receptor-neprilysin inhibitor (arni). J Clin Pharmacol. 2010;50:401–414 [PubMed: 19934029]

28. Bai HY, Mogi M, Nakaoka H, Kan-No H, Tsukuda K, Chisaka T, Wang XL, Kukida M, Shan BS, Yamauchi T, Higaki A, Iwanami J, Horiuchi M. Pre-treatment with lcz696, an orally active angiotensin receptor neprilysin inhibitor, prevents ischemic brain damage. Eur J Pharmacol. 2015;762:293–298 [PubMed: 26057694]

29. Suematsu Y, Miura S, Goto M, Matsuo Y, Arimura T, Kuwano T, Imaizumi S, Iwata A, Yahiro E, Saku K. Lcz696, an angiotensin receptor-neprilysin inhibitor, improves cardiac function with the attenuation of fibrosis in heart failure with reduced ejection fraction in streptozotocin-induced diabetic mice. Eur J Heart Fail. 2016;18:386–393 [PubMed: 26749570]

30. Burke RM, Lighthouse JK, Quijada P, Dirkx RA, Jr., Rosenberg A, Moravec CS, Alexis JD, Small EM. Small proline-rich protein 2b drives stress-dependent p53 degradation and fibroblast proliferation in heart failure. Proc Natl Acad Sci U S A. 2018;115:E3436–E3445 [PubMed: 29581288]

31. Trembley MA, Velasquez LS, de Mesy Bentley KL, Small EM. Myocardin-related transcription factors control the motility of epicardium-derived cells and the maturation of coronary vessels. Development. 2015;142:21–30 [PubMed: 25516967]

32. Moore-Morris T, Guimaraes-Camboa N, Banerjee I, Zambon AC, Kisseleva T, Velayoudon A, Stallcup WB, Gu Y, Dalton ND, Cedenilla M, Gomez-Amaro R, Zhou B, Brenner DA, Peterson KL, Chen J, Evans SM. Resident fibroblast lineages mediate pressure overload-induced cardiac fibrosis. J Clin Invest. 2014;124:2921–2934 [PubMed: 24937432]

33. Ivey MJ, Kuwabara JT, Pai JT, Moore RE, Sun Z, Tallquist MD. Resident fibroblast expansion during cardiac growth and remodeling. J Mol Cell Cardiol. 2018;114:161–174 [PubMed: 29158033]
34. Spindel ON, Burke RM, Yan C, Berk BC. Thioredoxin-interacting protein is a biomechanical regulator of src activity: Key role in endothelial cell stress fiber formation. Circ Res. 2014;114:1125–1132 [PubMed: 24515523]
35. Kanisicak O, Khalil H, Ivey MJ, Karch J, Maliken BD, Correll RN, Brody MJ, SC JL, Aronow BJ, Tallquist MD, Molkentin JD. Genetic lineage tracing defines myofibroblast origin and function in the injured heart. Nat Commun. 2016;7:12260 [PubMed: 27447449]
36. Shi J, Wang X, Nguyen J, Wu AH, Bleske BE, Zhu HJ. Sacubitril is selectively activated by carboxylesterase 1 (ces1) in the liver and the activation is affected by ces1 genetic variation. Drug Metab Dispos. 2016;44:554–559 [PubMed: 26817948]
37. Benz PM, Blume C, Seifert S, Wilhelm S, Waschke J, Schuh K, Gertler F, Munzel T, Renne T. Differential vasp phosphorylation controls remodeling of the actin cytoskeleton. J Cell Sci. 2009;122:3954–3965 [PubMed: 19825941]
38. Sirotkin AV, Makarevich AV, Pivko J, Kotwica J, Genieser H, Bulla J. Effect of cgmp analogues and protein kinase g blocker on secretory activity, apoptosis and the camp/protein kinase a system in porcine ovarian granulosa cells in vitro. J Steroid Biochem Mol Biol. 2000;74:1–9 [PubMed: 11074350]
39. Bhowmick NA, Ghiassi M, Bakin A, Aakre M, Lundquist CA, Engel ME, Arteaga CL, Moses HL. Transforming growth factor-beta1 mediates epithelial to mesenchymal transdifferentiation through a rhoa-dependent mechanism. Mol Biol Cell. 2001;12:27–36 [PubMed: 11160820]
40. Raja SG. Evaluation of clinical efficacy of fasudil for the treatment of pulmonary arterial hypertension. Recent Pat Cardiovasc Drug Discov. 2012;7:100–104 [PubMed: 22670803]
41. Rolli-Derkinderen M, Sauzeau V, Boyer L, Lemichez E, Baron C, Henrion D, Loirand G, Pacaud P. Phosphorylation of serine 188 protects rhoa from ubiquitin/proteasome-mediated degradation in vascular smooth muscle cells. Circ Res. 2005;96:1152–1160 [PubMed: 15890975]
42. McMurray JJ, Packer M, Desai AS, Gong J, Lefkowitz MP, Rizkala AR, Rouleau JL, Shi VC, Solomon SD, Swedberg K, Zile MR. Angiotensin-neprilysin inhibition versus enalapril in heart failure. N Engl J Med. 2014;371:993–1004 [PubMed: 25176015]
43. Tyler JM, Teerlink JR. The safety of sacubitril-valsartan for the treatment of chronic heart failure. Expert Opin Drug Saf. 2017;16:257–263 [PubMed: 28060547]
44. von Lueder TG, Wang BH, Kompa AR, Huang L, Webb R, Jordaan P, Atar D, Krum H. Angiotensin receptor neprilysin inhibitor lcz696 attenuates cardiac remodeling and dysfunction after myocardial infarction by reducing cardiac fibrosis and hypertrophy. Circ Heart Fail. 2015;8:71–78 [PubMed: 25362207]
45. Zimmermann A, Keller H. Effects of staurosporine, k 252a and other structurally related protein kinase inhibitors on shape and locomotion of walker carcinosarcoma cells. Br J Cancer. 1992;66:1077–1082 [PubMed: 1457347]

Commentary

What is new?

- We demonstrate that LCZ696 (Valsartan/sacubitril) treatment ameliorates maladaptive remodeling and fibrosis in a mouse model of left ventricle pressure overload.
- Valsartan/sacubitril directly reduces the pathologic accumulation of cardiac fibroblasts in vitro and in vivo.
- Valsartan/sacubitril blocks myofibroblast activation and the induction of pro-fibrotic genes.
- Mechanistically, sacubitrilat functions at least in part by preventing TGF-βI/AngII-dependent suppression of PKG signaling in cardiac fibroblasts.

What are the clinical implications?

- The clinical efficacy of Entresto in heart failure patients with reduced ejection fraction cannot be fully explained by the reduction in systemic blood pressure by the combination of angiotensin receptor blockade and increased ANP levels.
- Our study suggest the clinical efficacy of Entresto may partially stem from the direct amelioration of cardiac fibroblast activation and the development of fibrosis by blocking pathological suppression of PKG signaling.
- Our results suggest that Entrestro may prove useful in ameliorating cardiac fibrosis and diastolic dysfunction in heart failure patients with preserved ejection fraction.

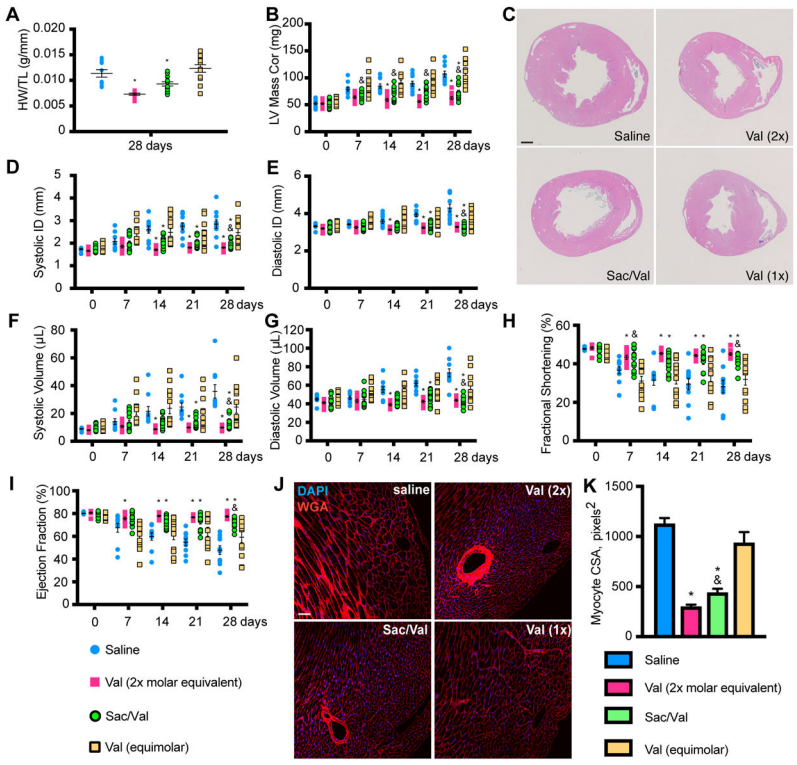

Figure 1: SAC/VAL prevents cardiac hypertrophy and loss of function associated with pressure overload-induced heart failure more effectively than equimolar valsartan.

A. Heart weight/tibia length ratio reveals a decrease in pressure overload-induced cardiac hypertrophy with SAC/VAL, which significantly reduces hypertrophy relative to saline or equimolar valsartan alone. n = 10, 10, 12, 14. One-way ANOVA with Tukey's multiple comparisons test. B. LV mass by echo confirms the significant effect of SAC/VAL relative to equimolar valsartan. For A, B, D-I: n = 10, 10, 12, 14. Two-way ANOVA with repeated measures (time). * = $p < 0.05$ compared to saline; & = $p < 0.05$ for SAC/VAL compared to equimolar valsartan. C. H&E staining of transverse sections through the papillary muscle further confirms SAC/VAL's significant effect against hypertrophic remodeling in response to pressure overload. Scale bar = 1mm. D-E. Systolic/diastolic LV internal diameter (ID) increase is prevented by SAC/VAL but not the molar equivalent of valsartan. F-G. Systolic/diastolic volume increase is prevented by SAC/VAL but not the molar equivalent of valsartan. Two-way ANOVA with repeated measures (time). H. Fractional shortening is significantly improved by SAC/VAL, but not the molar equivalent of valsartan. Two-way ANOVA with repeated measures (time). I. Ejection fraction is significantly improved by SAC/VAL but not the molar equivalent of valsartan. Two-way ANOVA with repeated measures (time). J. Myocyte cross sectional area (CSA) is visualized by wheat germ agglutinin (WGA) staining. Scale bar = 100 μm. K. CSA is increased due to concentric hypertrophic remodeling induced by pressure overload (saline), and is decreased in SAC/VAL-treated mice significantly more so than equimolar valsartan. One-way ANOVA, Tukey's multiple comparisons test. n = 5, 5, 6, 7. * = $p < 0.05$ compared to saline; & = $p < 0.05$ for SAC/VAL compared to equimolar valsartan.

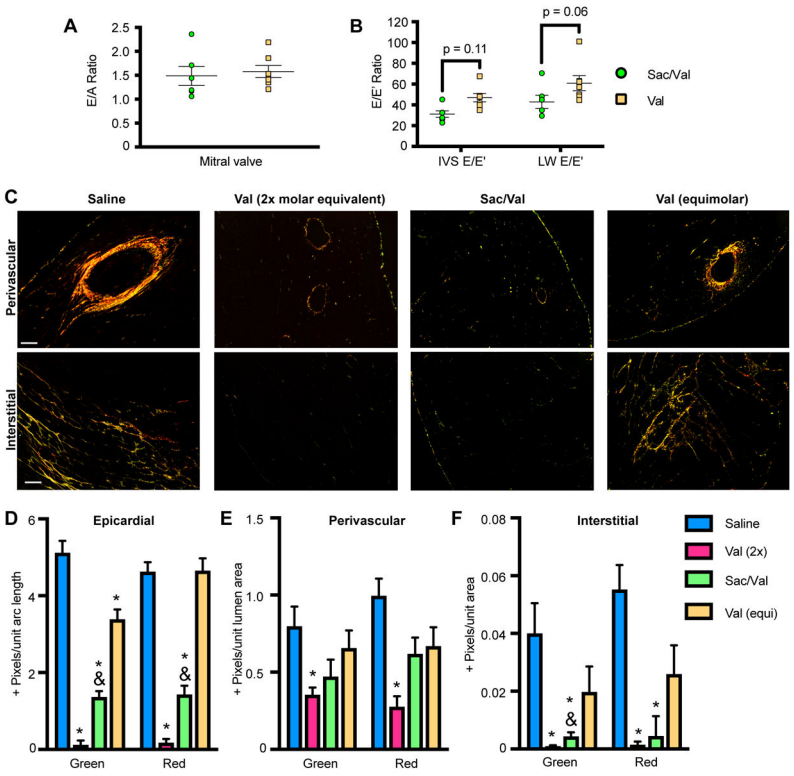

Figure 2: SAC/VAL treatment more effectively reduces cardiac fibrosis in response to pressure overload than equimolar valsartan.

A. E/A ratio is not statistically distinct between SAC/VAL- and valsartan-treated animals (28 days post-TAC). n = 12, 14. Student's unpaired t-test with Welch's correction. B. E/E' ratio (measured at mitral valve and intraventricular septum), trends lower (IVS: p = 0.11, MV: p = 0.06) in SAC/VAL-treated animals as compared to equimolar valsartan-treated animals. n = 12, 14. Student's unpaired t-test with Welch's correction. C. Heart sections were stained with PicroSirius Red and imaged with polarized light to visualize the deposition of fibrotic extracellular matrix. SAC/VAL significantly ameliorates fibrosis relative to saline, while the equivalent dose of valsartan does not. Scale bar = 200 μm D-F. Quantification of fibrosis in the epicardial, perivascular, and interstitial areas. Both green (thin/new) and red (thick/established) fibers were analyzed. n = 5, 5, 6, 7. Two-way ANOVA (independent variables green/new and red/established) with Tukey's multiple comparisons test. * = $p < 0.05$ compared to saline; & = $p < 0.05$ for SAC/VAL compared to equimolar valsartan.

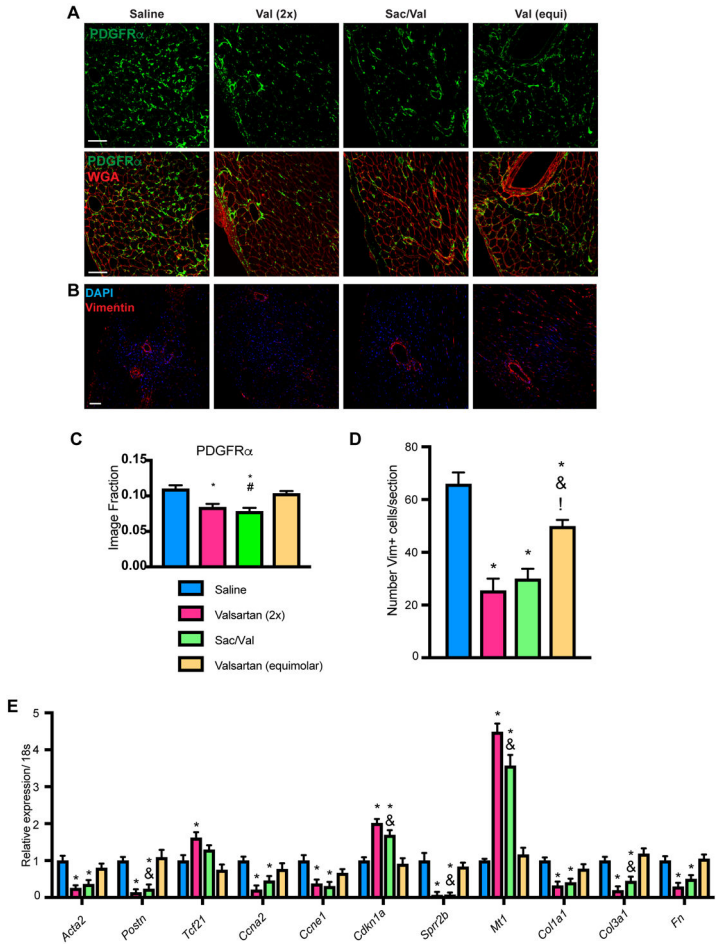

Figure 3: SAC/VAL attenuates accumulation of vimentin$^+$ and PDGFRα$^+$ cell populations, and isolated CF from SAC/VAL-treated hearts show significantly altered gene expression.

A. Staining for PDGFRα and WGA reveals that SAC/VAL significantly decreases CF load post-pressure overload relative to equimolar valsartan. Scale bar = 50μm. B. Sections stained for vimentin revealed that DAPI$^+$/vimentin$^+$ cell population expansion is significantly prevented by SAC/VAL as well as the equivalent dose of valsartan. Scale bar = 100 μm. B. Quantification of PDGFRα staining. One-way ANOVA with Tukey's multiple comparisons test. * = $p < 0.05$ compared to saline; & = $p < 0.05$ for SAC/VAL compared to equimolar valsartan. D. Quantification of vimentin staining, which confirms that while equimolar valsartan decreases fibroblast number, SAC/VAL is significantly more effective. n = 5, 5, 6, 7. One-way ANOVA with Tukey's multiple comparisons test. * = $p < 0.05$ compared to saline; & = $p < 0.05$ for SAC/VAL compared to equimolar valsartan. E. qRT-PCR for gene expression in fibroblasts isolated by Langendorff perfusion of mouse hearts reveals that SAC/VAL effectively targets proliferation, activation, and extracellular matrix-associated gene expression. The equivalent dose of valsartan has no statistically significant effect on any of these genes, while SAC/VAL confers significant changes that reflect a less pathologic gene program. n = 5, 5, 6, 7. Two-way ANOVA, Tukey's multiple comparisons test. * = $p < 0.05$ compared to saline; & = $p < 0.05$ for SAC/VAL compared to equimolar valsartan.

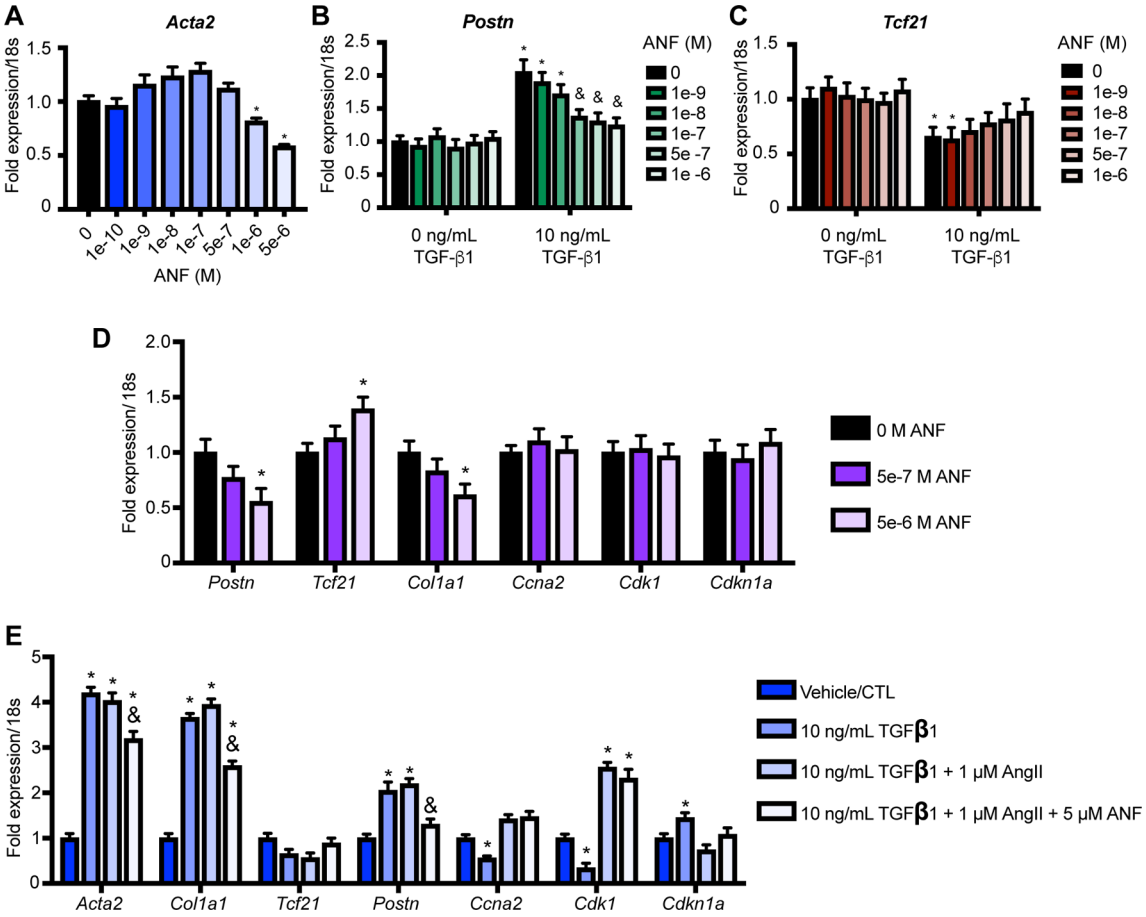

Figure 4: Treatment of CF with exogenous ANF causes dose-dependent decreases in myofibroblast gene expression.

A-B. Pre-treatment of neonatal mouse CF with ANF significantly and dose-dependently attenuates TGF-β1 dependent induction of *Acta2* (A) and *Postn* (B) gene expression. C. ANF pre-treatment trends toward recovery of *Tcf21* expression. For all experiments, n = 3 each condition. One-way ANOVA with repeated measures (ANF concentration). * = $p < 0.05$ relative to 0ng/mL TGF-β1 / 0 M ANF. & = $p < 0.05$ relative to 10ng/mL TGF-β1 / 0 M ANF. D. ANF pre-treatment does not significantly alter cell cycle gene expression in neonatal CF that are stimulated with TGF-β1 alone. One-way ANOVA for each gene with repeated measures (concentration). * = $p < 0.05$ relative to vehicle control. E. ANF significantly ablates TGF-β1 / AngII-induced changes in cell cycle gene expression that are associated with proliferation. Two-way ANOVA with Tukey's multiple comparisons test. * = $p < 0.05$ compared to vehicle control. & = $p < 0.05$ relative to TGF-β1/AngII condition.

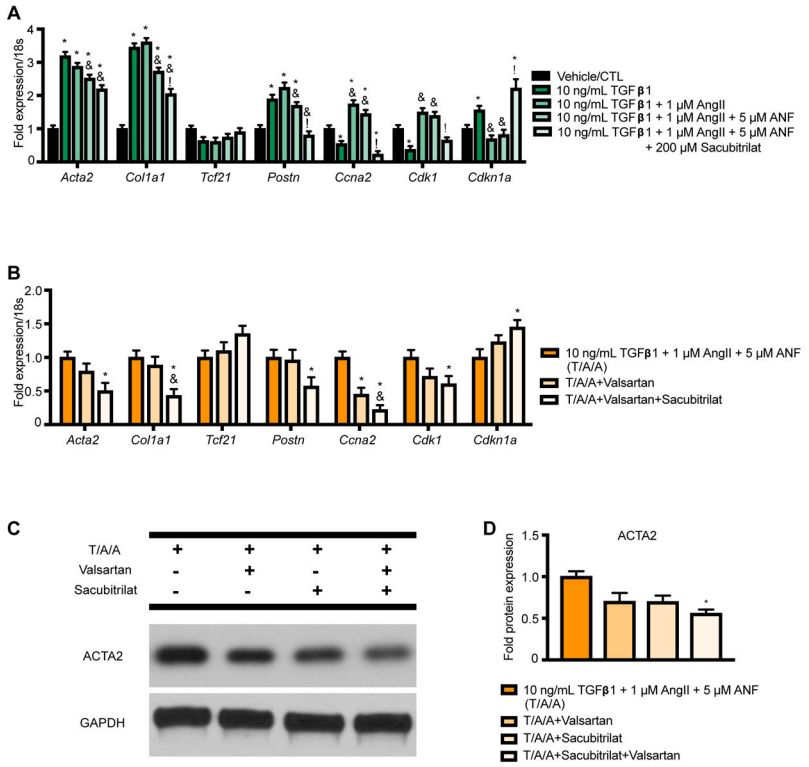

Figure 5: Sacubitrilat ameliorates expression of myofibroblast markers in TGF-β1/AngII/ANF-stimulated nCF.

A. Pretreatment with Sacubitrilat significantly decreases activation- and proliferation-associated gene expression in response to TGF-β1/AngII/ANF stress stimulus in neonatal CF. n = 3 each condition for all experiments. Two-way ANOVA with Tukey's multiple comparisons test. * = $p < 0.05$ relative to vehicle control. & = $p < 0.05$ relative to the TGF-β1/AngII condition. ! = $p < 0.05$ relative to the TGF-β1/AngII/ANF condition. B. Pretreatment with valsartan alone only significantly alters proliferation-associated gene expression in neonatal CF, while valsartan + sacubitrilat also significantly inhibits some activation-associated genes. Two-way ANOVA with Tukey's multiple comparisons test. * = $p < 0.05$ relative to vehicle control. & = $p < 0.05$ relative to the TGF-β1/AngII/ANF/valsartan condition. C. Valsartan and Sacubitrilat significantly inhibit ACTA2 induction by TGF-β1/AngII/ANF. One-way ANOVA with Tukey's multiple comparison test. * = $p < 0.05$ relative to TGF-β1/AngII/ANF.

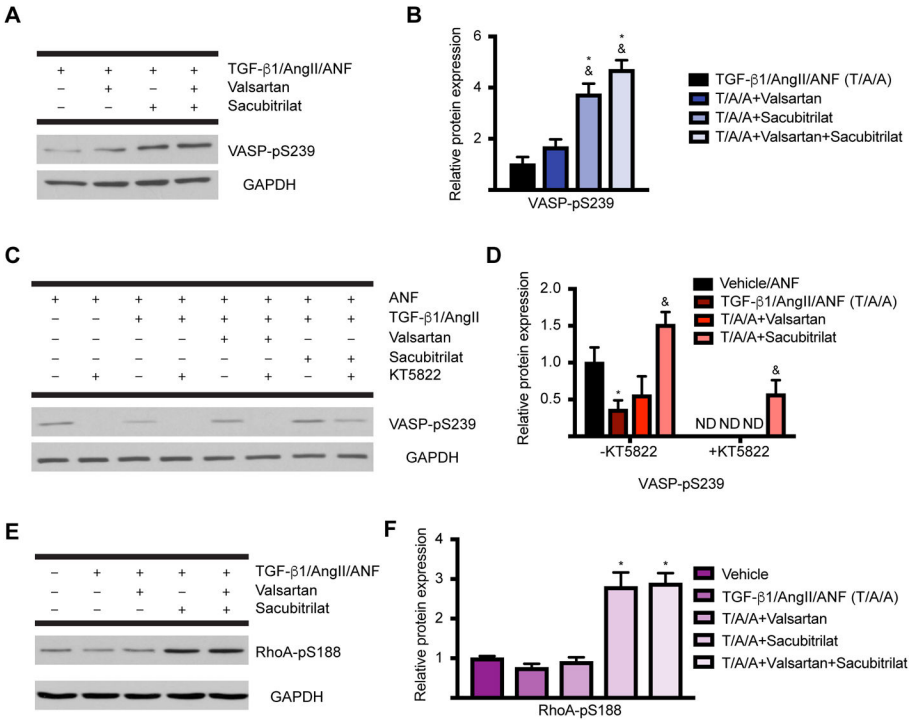

Figure 6: Sacubitrilat stabilizes PKG signaling and inhibits RhoA in activated CF.

A. Sacubitrilat alone or in combination with valsartan promotes the PKG-dependent phosphorylation of VASP at S239. B. Quantification of (A). n = 3 for each condition for all experiments. One-way ANOVA with Tukey's multiple comparisons test. * = $p < 0.05$ relative to TGF-β1/AngII/ANF, & = $p < 0.05$ relative to TGF-β1/AngII/valsartan. C. Use of the PKG inhibitor KT5822 confirms that Sacubitrilat effects are transduced primarily through PKG. D. Quantification of (C). Two-way ANOVA with Tukey's multiple comparisons test. * = $p < 0.05$ relative to vehicle/ANF, & = $p < 0.05$ relative to TGF-β1/AngII/ANF; ND, not detected. E. Sacubitrilat promotes the PKG-dependent phosphorylation of RhoA at S188, which inactivates RhoA (a major transducer of myofibroblast activation). F. Quantification of (E). One-way ANOVA with Tukey's multiple comparisons test. * = $p < 0.05$ compared to vehicle.

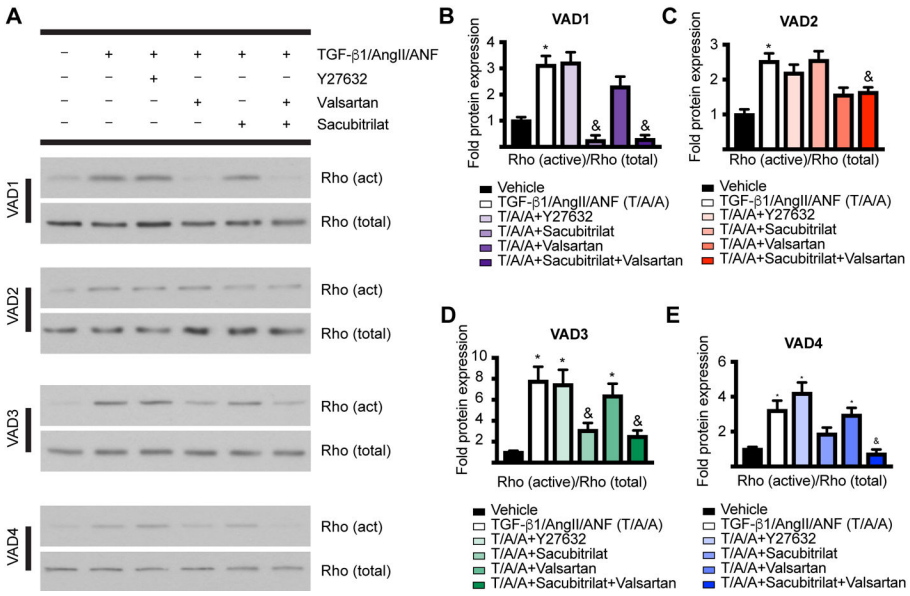

Figure 7: SAC/VAL is more efficient at inactivating Rho than is SAC or VAL alone in CF derived from heart failure patients.

A. Pulldown of Rho with beads conjugated to the Rho-binding domain of rhotekin (specific for activated Rho) reveals that for all four patient-derived primary CF lines tested, the combination of Sacubitrilat and valsartan significantly ameliorates Rho activation. B-E. Quantification of data for each line isolated as shown in (A). n = 3 each condition. One-way ANOVA for each patient-derived line, Tukey's multiple comparisons test. * = $p < 0.05$ relative to vehicle. & = $p < 0.05$ relative to TGF-β1/AngII/ANF.